International Transaction Journal of Engineering, Management, & Applied Sciences & Technologies

http://www.TuEngr.com, http://go.to/Research

An Investigation on Patrol Robot Coverage Performance Based on Chaotic and non Chaotic Guiding Signals

Ashraf Anwar [a*] **and Hedi Khammari** [a]

[a] *Department of Computer Engineering, Faculty of Computers and Information Technology, Taif University, SAUDIA ARABIA*

ARTICLEINFO

Article history:
Received 20 July 2011
Received in revised form 08 September 2011
Accepted 09 September 2011
Available online 12 September 2011

Keywords:
Mobile robot, chaotic motion, chaotic mobile robot, Chua's circuit, instable focus.

ABSTRACT

In some practical applications of the mobile robot, it is expected to ensure the fullest coverage of a certain area with or without obstacle avoidance. This paper shows that both chaotic and non chaotic signals can be advantageous for providing good coverage performance. Our study includes, in addition to parameters adjusting and mapping the appropriate chaotic variables to robot's kinematic variables, a comparison of the coverage performance generated by three different behaviors of Chua's circuit. These behaviors include an instable focus and two chaotic signals having single scroll and double scroll shaped phase portraits respectively.

Contrary to a commonly held belief, a non-chaotic behavior can lead to generate complex trajectories of a mobile robot and to provide better coverage performance. Such behavior is an instable focus which is a repeller, obtained by using a particular parameter set of Chua's circuit.

1. Introduction

Chaos is one of the mysterious phenomena ever discovered in the behavior of nonlinear dynamical systems. Such phenomenon which is highly sensitive to initial conditions and

*Corresponding author (**Ashraf Anwar**). E-mail address: ashrafmanwar90@yahoo.com. ©2011 International Transaction Journal of Engineering, Management, & Applied Sciences & Technologies. Volume 2 No.4. ISSN 2228-9860. eISSN 1906-9642. Online Available at http://TuEngr.com/V02/405-421.pdf

happens even in deterministic systems has been studied deeply in several physical and sociological fields, then becoming a multidisciplinary issue.

A robot following a chaotic path, generated by the Arnold's equation, was introduced for the first time in (Nakamura et al., 2001, Sekiguchi, et al., 1999). In other studies it has been reported that Chua's patterns are more suitable to chaotic robots for different reasons namely the low cost, the availability and the largest coverage areas (Jansri et al., 2004, Sooraksa, et al., 2010).

In many applications, control of mobile robots designed to perform specific tasks are generated by chaotic signals (Nakamura et al., 2001, Sekiguchi et al., 1999, Jansri et al., 2004, Sooraksa et al., 2010, Martins-Filho, 2004, Martins et al., 2007, Palacin, 2004, Islam et al., 2005, Nehmzow, 2003).

The main purpose of our study is to find out the highest performance coverage areas for different sets of Chua circuit parameters. Is chaotic signal is a unique alternative to ensure maximum and fast coverage areas? Are there any non-chaotic patterns that can achieve the same coverage performances? These are among the questions that represent the main issue of this paper.

Two performance indexes are used to evaluate the coverage areas of the chaotic mobile robot, namely a performance index k representing a ratio of areas that the trajectory passes through over the total working area and an evenness index E which refers in general to how close in numbers each species in an environment are. In our case study the robot workspace is split into four quarters which represent the so called species.

Not only large coverage areas are desirable in certain applications of mobile robot, but also coverage speed and eventually the shortest path traveled by the robot. The complexity of chaotic motion is increased by the multiple reflections of the robot trajectory on the workspace boundaries and obstacles.

In this paper we restrict our study to generate traveling paths from Chua's circuit state variables and to consider a rectangular workspace without obstacles.

Large coverage areas are desirable for many applications such as robots designed for scanning of unknown workspaces with borders and barriers of unknown shape, as in patrol for exploring an unknown mine-filled terrain or cleaning purposes. The Chua's pattern is the most interesting one among other candidate's patterns due to its largest coverage areas, low cost, and ease for implementation (Sooraksa et al., 2010). Aiming to fulfill the requirements of high coverage coefficient and high evenness index of a specified area crossed far and wide erratically by the mobile robot, we focus our work on investigation of Chua's circuit parameters sets and the appropriate mapping of the state variables to robot's kinematic variables and compute the performance indexes.

Some experimental and theoretical studies have focused on the chaotic motion of the robot without considering the coverage performance (Sekiguchi et al., 1999, Chanvech, 2006, Martins et al., 2006) where as in other studies, it has been reported that a large coverage area is among the most important performances that may characterize the mobile robot motion (Jansri et al., 2004).

The paper structure is as follows: The next section presents some general reminders about the Chua's circuit and the mobile robot model. Section 3 is dedicated to describe the methodology which includes the integration of Chua's circuit equations to mobile robot model, and the performance criteria to be applied. Section 4 is reserved to the simulation results. Finally section 5 concludes this paper.

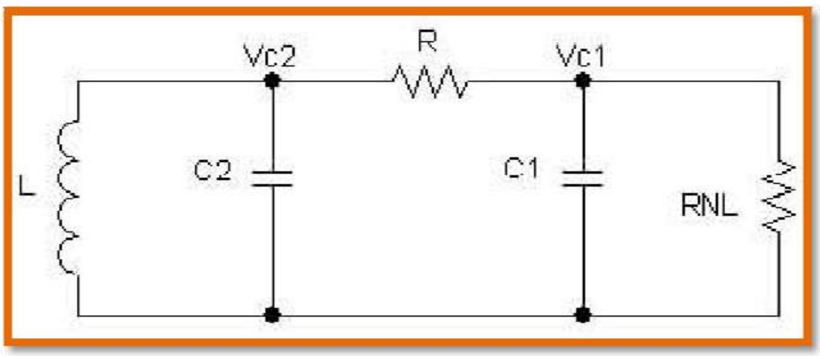

Figure 1: Equivalent Chua's circuit**.**

*Corresponding author (**Ashraf Anwar**). E-mail address: ashrafmanwar90@yahoo.com. International Transaction Journal of Engineering, Management, & Applied Sciences & Technologies. Volume 2 No.4. ISSN 2228-9860. eISSN 1906-9642. Online Available at http://TuEngr.com/V02/405-421.pdf

2. Background

2.1 Chua's circuit

The Chua’s circuit is of interest to nonlinear scientists from different disciplines, it includes two capacitors, one inductance a linear resistor and a non-linear resistor known as Chua’s diode, see Figure 1, (Leon, 2007).

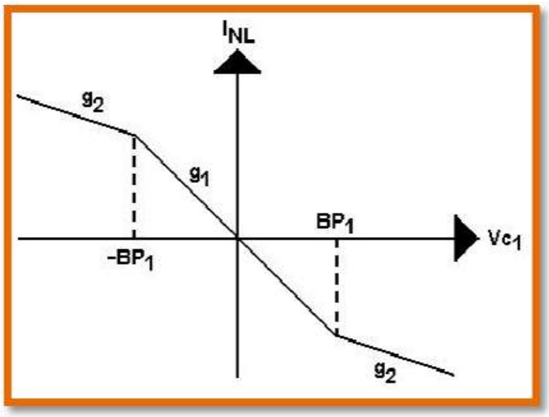

Figure 2: Chua's diode I-V characteristic.

Knowing the Chua's diode I-V piecewise-linear characteristic given by Figure 2, where $\boldsymbol{g_1}$ denotes the slope of the middle segment and $\boldsymbol{g_2}$ denotes the slope of the two outer segments, the non-linear part of the circuit can be solved by the following system of equations:

$$I_{NL}= \begin{cases} -g_2 V_{c1} + (g_1 - g_2) BP_1, & V_{c1} < -BP_1 \\ -g_1 V_{c1} & -BP_1 \leq V_{c1} \leq BP_1 \\ -g_2 V_{c1} + (g_2 - g_1) BP_1, & V_{c1} > BP_1 \end{cases} \qquad (1)$$

The state space equations describe the relations between the capacitor voltages $V_{c1} and\ V_{c2}$, the inductance current I_L and its derivatives. The compact form of these expressions is:

$$\begin{bmatrix} \dot{V_{c1}} \\ \dot{V_{c2}} \\ \dot{I_L} \end{bmatrix} = A \begin{bmatrix} V_{c1} \\ V_{c2} \\ I_L \end{bmatrix} + b \qquad (2)$$

The Circuit behavior is then described by the following differential system:

$$\begin{bmatrix} \dot{V_{c1}} \\ \dot{V_{c2}} \\ \dot{I_L} \end{bmatrix} = \begin{bmatrix} \frac{-1}{RC1} + \frac{g_2}{C1} & \frac{1}{RC1} & 0 \\ \frac{1}{RC2} & \frac{-1}{RC2} & \frac{1}{C2} \\ 0 & \frac{-1}{L} & 0 \end{bmatrix} \begin{bmatrix} V_{c1} \\ V_{c2} \\ I_L \end{bmatrix} + \begin{bmatrix} \frac{(g_2-g_1)}{C1} \\ 0 \\ 0 \end{bmatrix} \qquad V_{C1<-BP_1} \qquad (3)$$

$$\begin{bmatrix} \dot{V_{c1}} \\ \dot{V_{c2}} \\ \dot{I_L} \end{bmatrix} = \begin{bmatrix} \frac{-1}{RC1} + \frac{g_1}{C1} & \frac{1}{RC1} & 0 \\ \frac{1}{RC2} & \frac{-1}{RC2} & \frac{1}{C2} \\ 0 & \frac{-1}{L} & 0 \end{bmatrix} \begin{bmatrix} V_{c1} \\ V_{c2} \\ I_L \end{bmatrix} + \begin{bmatrix} \frac{(g_2-g_1)}{C1} \\ 0 \\ 0 \end{bmatrix} \qquad -BP_1 \leq V_{C1} \leq Bp_1 \qquad (4)$$

$$\begin{bmatrix} \dot{V_{c1}} \\ \dot{V_{c2}} \\ \dot{I_L} \end{bmatrix} = \begin{bmatrix} \frac{-1}{RC1} + \frac{g_2}{C1} & \frac{1}{RC1} & 0 \\ \frac{1}{RC2} & \frac{-1}{RC2} & \frac{1}{C2} \\ 0 & \frac{-1}{L} & 0 \end{bmatrix} \begin{bmatrix} V_{c1} \\ V_{c2} \\ I_L \end{bmatrix} + \begin{bmatrix} \frac{(g_1-g_2)}{C1} \\ 0 \\ 0 \end{bmatrix} \qquad V_{C1>BP_1} \qquad (5)$$

The phase trajectories are obtained by solving the ordinary differential equations (ODE) in three different regions using an adequate numerical method such as Forward Euler (FE).

The FE method states that:

$$X_{n+1} = X_n + h\, f(x_n, t_n) \qquad (6)$$

Where X_{n+1} is the solution of the ODE at time t_{n+1}, X_n is the current value, and h is the step-size.

Using (6) to solve (2) we obtain:

$$X_{n+1} = X_n + h\,(Ax_n + b) \qquad (7)$$

2.2 The mobile robot model

The robot is supposed to operate on a horizontal plane with a motion described in terms of

*Corresponding author (**Ashraf Anwar**). E-mail address: ashrafmanwar90@yahoo.com. International Transaction Journal of Engineering, Management, & Applied Sciences & Technologies. Volume 2 No.4. ISSN 2228-9860. eISSN 1906-9642. Online Available at http://TuEngr.com/V02/405-421.pdf

linear velocity v(t) and direction θ(t), describing an instantaneous linear motion of the medium point of the wheel axis and a rotational motion (rotational velocity $\boldsymbol{\omega}$(t)) of the robot body over this same point. The geometry of the mobile robot's motion on Cartesian plane is given in Figure 3.

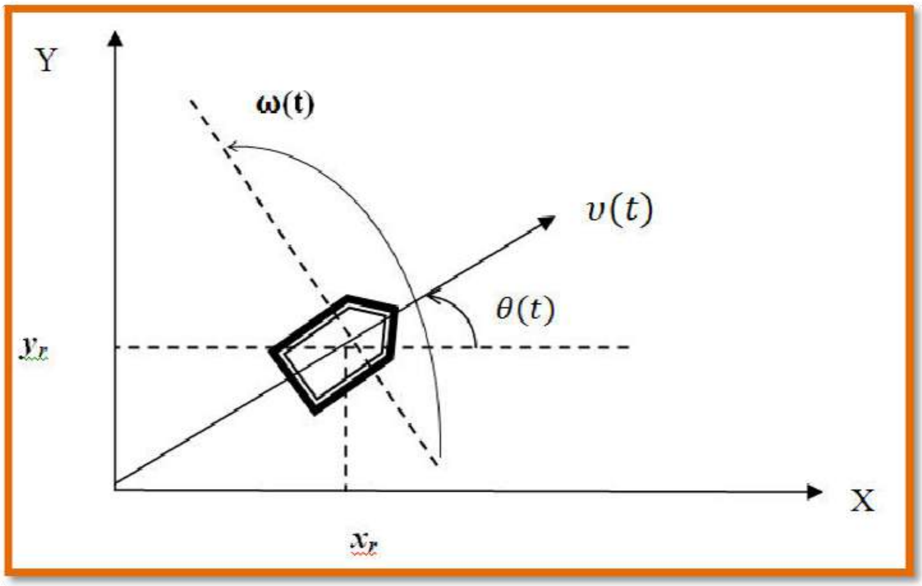

Figure 3: Geometry of the robot motion on Cartesian plane**.**

The mathematical model of this motion considers two control variables (v, w) and three state variables: the robot position and orientation (x_r(t), y_r(t), θ(t)):

$$\begin{bmatrix} \dot{x}_r \\ \dot{y}_r \\ \dot{\theta} \end{bmatrix} = \begin{bmatrix} \cos\theta & 0 \\ \sin\theta & 0 \\ 0 & 1 \end{bmatrix} \begin{bmatrix} v \\ \omega \end{bmatrix} \tag{8}$$

3. Methodology

3.1 Integration of the Chua's equation

In order to integrate the Chua's circuit into the controller of the mobile robot, we consider the following state variables:

$$\boldsymbol{x_1} \equiv \boldsymbol{V_{c1}} \qquad \boldsymbol{x_2} \equiv \boldsymbol{V_{c2}}, \qquad \boldsymbol{x_3} \equiv \boldsymbol{I_L} \tag{9}$$

From equation (2) the set of equations of Chua's circuit become:

$$\begin{bmatrix} \dot{x_1} \\ \dot{x_2} \\ \dot{x_3} \end{bmatrix} = \boldsymbol{A} \begin{bmatrix} x_1 \\ x_2 \\ x_3 \end{bmatrix} + \boldsymbol{b} \tag{10}$$

Consequently, the state equation of the chaotic mobile robot after integrating the set of equations of Chua's circuit with the mathematical model of the mobile robot equation (**8**), we obtain the following system of equations:

$$\begin{bmatrix} \dot{x_1} \\ \dot{x_2} \\ \dot{x_3} \\ \dot{x_r} \\ \dot{y_r} \end{bmatrix} = \begin{bmatrix} \boldsymbol{A} \begin{bmatrix} x_1 \\ x_2 \\ x_3 \end{bmatrix} + \mathbf{b} \\ v \cos(\theta) \\ v \sin(\theta) \end{bmatrix} \tag{11}$$

The corresponding mapping parameters from 3-D chaotic circuit into 2-D one is as follows:

Table 1: Mapping chaotic variables to robot's kinematic variables, where θ corresponds to the orientation angle of the mobile robot.

System	θ
Case 1	x_1
Case 2	x_2
Case 3	x_3

3.2 Evaluation criteria

The evaluation criteria are set according to the application purpose. Since we would like to use the robot in wandering around an area of no maps, the chaotic trajectory should cover the entire areas of patrolling as much as possible. In the following two performance criteria are to be considered to evaluate the coverage rate of the chaotic mobile robot, namely the performance index *K* and the evenness index *E*.

*Corresponding author (**Ashraf Anwar**). E-mail address: ashrafmanwar90@yahoo.com.

3.2.1 A performance index K representing a ratio of areas that the trajectory passes through or used space (A_u), over the total working area (A_t)

$$K = \frac{A_u}{A_t} \tag{12}$$

Similarly, let us consider a rectangular shaped area, (see Figure 5), the total area can be split into four quarters, denoted Q=1, 2, 3, 4. For each quarter the quantitative measurement of the trajectory can be evaluated by using the following equation:

$$K_Q = \frac{A_{uQ}}{A_{tQ}} \tag{13}$$

K_Q being the performance index of the Q^{th} quadrant, A_{uQ} is the area crossed by the trajectory in the Q^{th} quadrant. In our case, we have

$$A_{tQ} = \frac{A_t}{4} \tag{14}$$

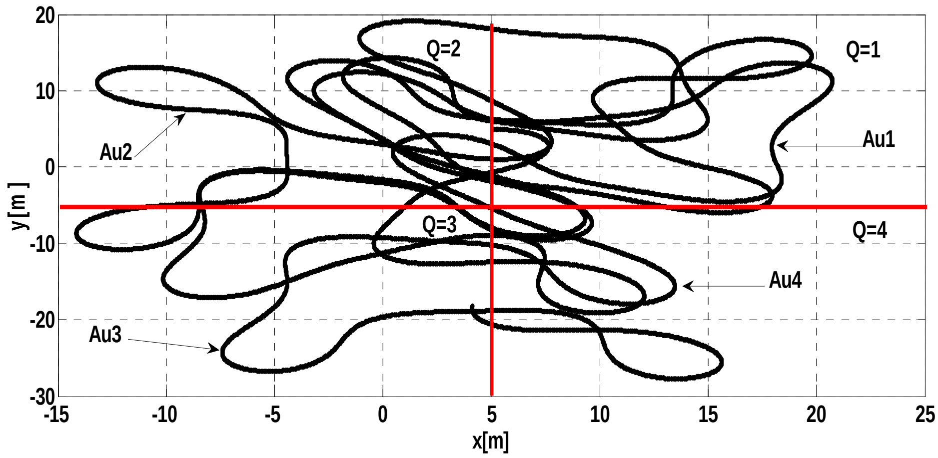

Figure 5: Partition of the specified area.

3.2.2 An evenness index E refers to how close in numbers each species in an environment are. The evenness index can be represented in our situation by (J. Nicolas, et al., 2003):

$$E = 1 - \frac{\sum_{Q=1}^{S} K_Q \ln (k_Q)}{\ln (s)} \tag{15}$$

Where s: is the number of specie, (in this case s = 4 Quarters). E is constrained between 0 and 1. The less variation in covering the areas between the species, the higher E is.

4. Simulation Results

The circuit simulation of the Chua's circuit, introduced in section 2 was built. The values used for the simulation were the following:

Table 2: Chua's circuit parameter settings.

C1	C2	L	$V_{c1}(0)$	$V_{c2}(0)$	$I_L(0)$	g_1	g_2	BP_1	h	R
450 pF	1.5nF	1mH	10^{-5}	0V	0A	1/1358	1/2464	0.114	10^{-7}	0.15-2 KΩ

Three different behaviors: Instable Focus, single scroll, and double scroll trajectories had been observed by changing the value of R from (150-2000) Ω.

Results presented in this paper aim to put into evidence that even with a non-chaotic trajectory we can obtain good coverage performances. For simplicity, an area of 20m x 20m is used as a workspace coverage trajectory in computer simulation. The robot moves as if is reflected by the boundary "mirror mapping".

The initial conditions were established as in Table 2 and the program was set to run a total of n=3000 iterations (for example) and robot speed is 1m/s. Simulations were performed for a set of resistor's values R in order to reveal the best values of performance index K and the evenness index E. The simulation results for the cases 1, 2 and 3, described in Table 1 are given in Tables 3, 4 and 5 respectively. Nevertheless, some important results are to be underlined to point out the fact that a non chaotic trajectory corresponding to an instable focus given in Figure 6 can lead to a higher an important coverage rate. Such attractor, obtained for R= 400 Ω. The performance indexes are even higher than those obtained for chaotic trajectories (K=88.64%, E=69.2%).

A double scroll attractor (Figure 7) was obtained for R= 1400 Ω. The robot trajectory generated by such chaotic attractor has a performance index K=86.76% and an Evenness index E=64.64%.

*Corresponding author (**Ashraf Anwar**). E-mail address: ashrafmanwar90@yahoo.com.

Table 3: Case 1 and run time for n=3000.

Resistance R[Ω]	% of K	% of Q=1	% of Q=2	% of Q=3	% of Q=4	% of E	Chua's pattern
150	82.53	94.86	79.21	71.01	85.04	55.59	Instable focus
200	74.44	58.71	67.44	91.75	79.86	39.63	Instable focus
300	84.90	95.64	82.56	74.78	86.63	60.88	Instable focus
400	88.64	91.01	88.33	86.30	88.91	69.20	Instable focus
500	69.79	81.17	48.14	55.79	94.08	34.77	Instable focus
600	80.63	82.03	93.89	78.24	68.36	51.41	Instable focus
700	83.98	81.46	87.04	86.48	80.94	57.84	Instable focus
800	85.00	83.34	88.52	86.61	81.54	60.27	Instable focus
900	83.81	90.62	81.54	77.23	85.83	57.71	Instable focus
1000	84.16	78.88	89.27	89.46	79.05	58.60	Instable focus
1100	82.80	85.18	82.80	80.45	82.76	54.96	Double scroll
1200	65.90	93.29	87.61	40.05	42.64	34.31	Double scroll
1300	80.69	69.76	76.80	92.35	83.88	51.32	Double scroll
1400	86.76	82.61	88.69	91.00	84.76	64.64	Double scroll
1500	81.62	76.43	71.10	86.24	92.70	53.42	Double scroll
1600	85.74	85.74	87.98	85.71	83.53	61.98	Double scroll
1700	82.08	86.83	84.36	77.43	79.70	53.47	Single scroll
1800	85.83	82.99	92.53	88.46	79.34	62.60	Single scroll
1900	84.44	80.49	76.28	88.06	92.92	59.51	Instable focus
2000	76.12	90.24	68.43	62.89	82.94	42.36	Instable focus

Table 4: Case 2 and run time for n= 3000.

Resistance R[Ω]	% of K	% of Q=1	% of Q=2	% of Q=3	% of Q=4	% of E	Chua's pattern
150	86.02	85.88	89.30	86.10	82.80	62.71	Instable focus
200	76.62	62.08	76.39	92.70	78.28	43.35	Instable focus
300	65.82	96.23	78.95	39.71	48.41	32.08	Instable focus
400	83.53	89.81	77.61	77.28	89.42	57.27	Instable focus
500	85.65	82.43	83.51	88.90	87.76	61.85	Instable focus
600	87.04	84.08	86.83	90.06	87.21	65.23	Instable focus
700	84.45	85.18	87.42	83.67	81.53	58.90	Instable focus
800	82.26	87.04	80.55	77.59	83.85	53.87	Instable focus
900	85.17	81.05	89.10	89.29	81.23	60.83	Instable focus
1000	80.36	91.76	87.89	69.37	72.42	50.97	Instable focus
1100	79.62	89.24	90.41	69.86	68.96	49.54	Double scroll
1200	84.25	86.68	78.85	81.68	89.80	58.66	Double scroll
1300	82.71	93.49	83.13	72.59	81.64	55.66	Double scroll
1400	81.05	70.50	75.58	92.15	85.95	52.15	Double scroll
1500	86.30	85.19	85.37	87.41	87.22	63.33	Double scroll
1600	84.81	81.92	78.80	87.54	91.00	60.08	Double scroll
1700	83.24	87.22	81.95	79.34	84.45	56.09	Single scroll
1800	84.90	81.71	87.54	88.11	82.25	60.06	Single scroll
1900	84.25	76.81	77.14	91.71	91.32	59.25	Instable focus
2000	76.72	90.81	69.39	63.53	83.15	43.54	Instable focus

Table 5: Case 3 and run time for n=3000.

Resistance R[Ω]	% of K	% of Q=1	% of Q=2	% of Q=3	% of Q=4	% of E	Chua's pattern
150	81.17	73.44	81.32	89.30	80.65	51.71	Instable focus
200	76.73	93.50	76.50	61.61	75.31	43.76	Instable focus
300	75.92	85.38	93.27	65.27	59.75	43.30	Instable focus
400	80.89	89.67	84.31	72.50	77.10	51.29	Instable focus
500	73.93	94.27	70.61	56.02	74.80	39.19	Instable focus
600	78.65	91.58	81.06	66.65	75.79	47.00	Instable focus
700	83.89	80.21	87.22	87.59	80.56	57.71	Instable focus
800	83.26	77.83	89.60	88.63	76.98	56.59	Instable focus
900	66.13	42.48	41.13	88.99	91.93	34.34	Instable focus
1000	80.88	83.77	71.63	77.49	90.63	51.37	Instable focus
1100	77.70	88.00	63.03	66.69	93.10	46.61	Double scroll
1200	73.13	85.34	90.39	60.07	56.71	38.37	Double scroll
1300	74.57	94.66	80.52	56.58	66.51	40.86	Double scroll
1400	76.57	68.75	71.39	84.64	81.51	41.86	Double scroll
1500	80.36	83.31	85.36	77.32	75.46	49.61	Double scroll
1600	73.09	68.16	55.41	75.69	93.10	37.55	Double scroll
1700	76.39	77.96	79.70	74.78	73.14	40.78	Single scroll
1800	44.81	70.51	55.46	23.45	29.82	8.08	Single scroll
1900	76.46	84.26	75.56	69.03	76.98	41.34	Instable focus
2000	43.78	50.55	28.70	34.73	61.17	1.09	Instable focus

A single scroll attractor given in Figure 8 was obtained for R= 1800Ω. The corresponding robot trajectory possesses also good coverage performances; (K=85.83%, E=62.6%).

The situations described above corresponding to three different phase portraits are extracted from Table 2 in which the robot θ(t) orientation is $\boldsymbol{V_{c1}}$, (case1). Thus, the complexity of the mobile robot motion can result either of a chaotic trajectory reflected on the external boundaries, or a non-chaotic trajectory which undergoes multiple reflections on such boundaries or obstacles. It is worth noting that the best performances in case 1 are obtained for R=400Ω. The corresponding phase portrait is that of an instable focus or a repeller.

In case 2, the best coverage performances are obtained for R=600Ω. The phase portrait is that of an instable focus or a repeller, K=87.04%, E=65.23%.

In case 3, the performance index K and the evenness index E are maximum for R= 700Ω. The phase portrait is that of an instable focus or a repeller, K=83.89%, E=57.71%.

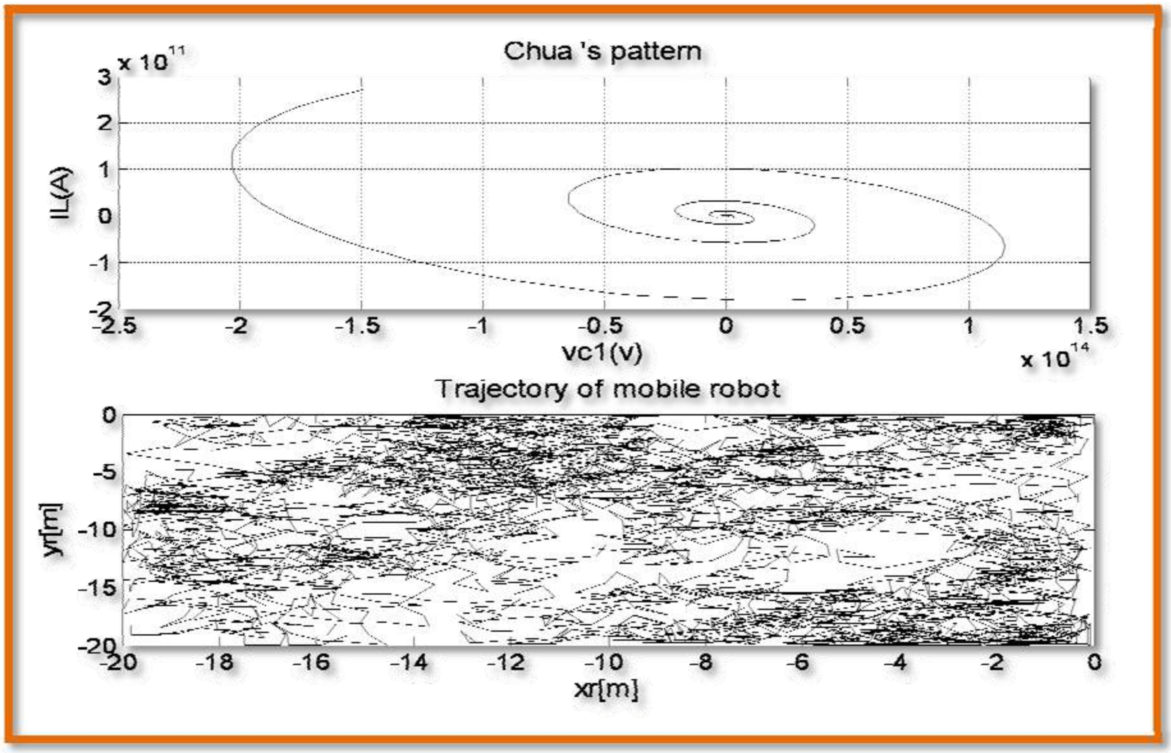

Figure 6: Chua's pattern (instable focus), and the corresponding trajectory at R=400, 'case 1'.

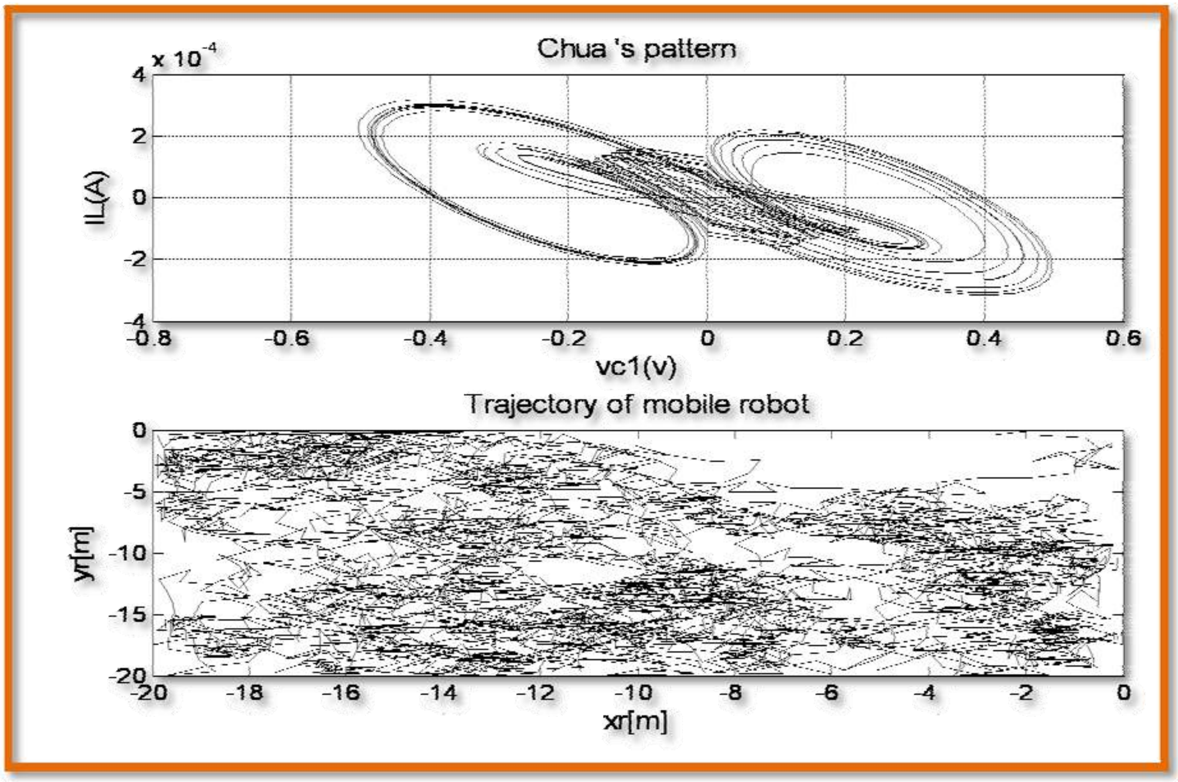

Figure 7: Chua's pattern (double scroll), and the corresponding trajectory at R=1400, 'case 1'

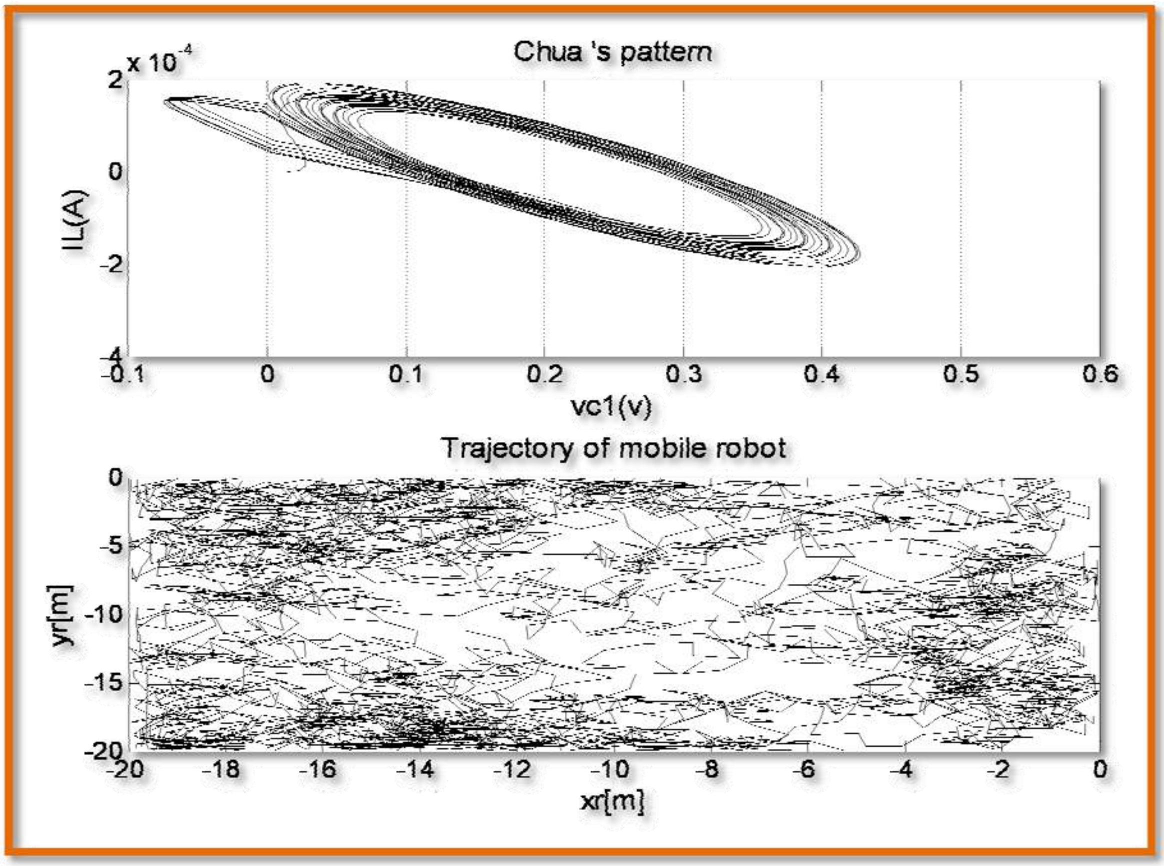

Figure 8: Chua's pattern (single scroll), and the corresponding trajectory at R=1800, 'case 1'.

To investigate the results at various runtime, we performed the following steps:

- The robot guided Chua's patterns (instable focus, single scroll, and double scroll), resulting from the three different cases at the specified values of the resistor R in each case Table 3, Table 4, and Table 5, are elaborated.
- We extracted the values of the resistor R which give maximum performance indices K and E in each Chua's pattern and in every case.
- We performed runtime ranging from n = 1000-10,000 iterations (simulation time) at the specified values of the resistor R for each Chua's pattern resulting in every case (step 2), and the results of the performance indices K and E are recorded.

The relations of the results of the performance indices K and E of the robot guided Chua's patterns as runtime ranging from 1000-10,000 iterations (simulation time) in case 1, case 2, and case 3, are depicted in Figure 9, Figure 10, and Figure 11 respectively.

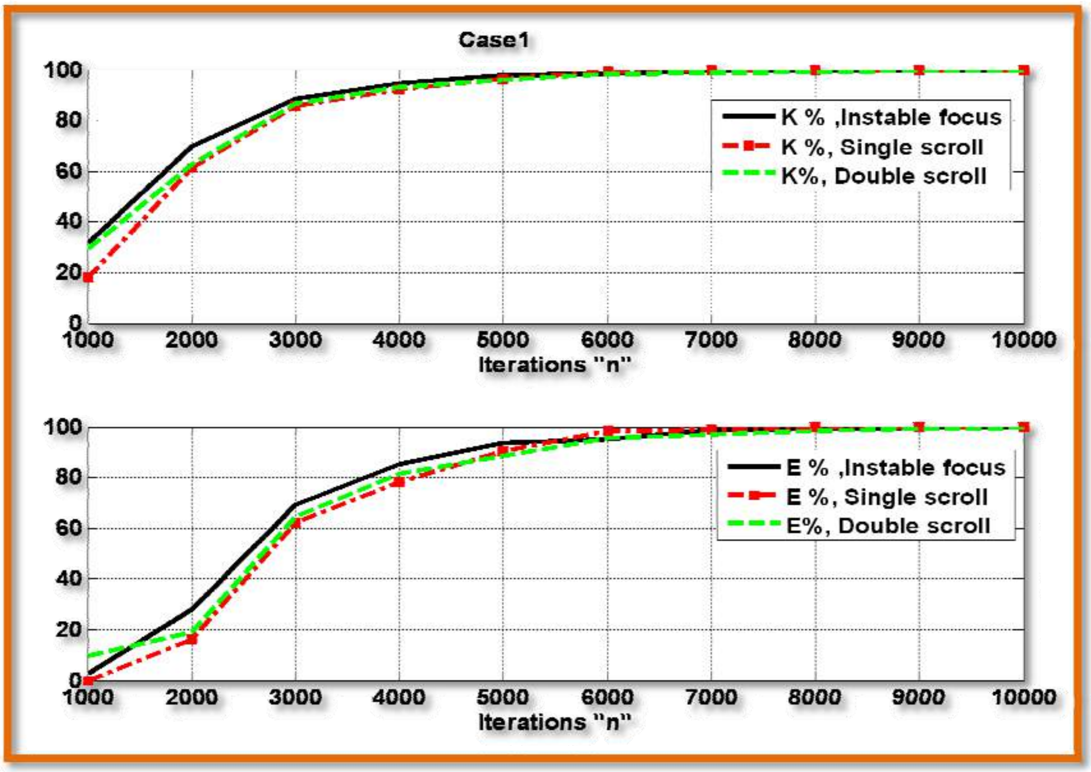

Figure 9: Performance indices K and E of the Chua's patterns versus time, case 1.

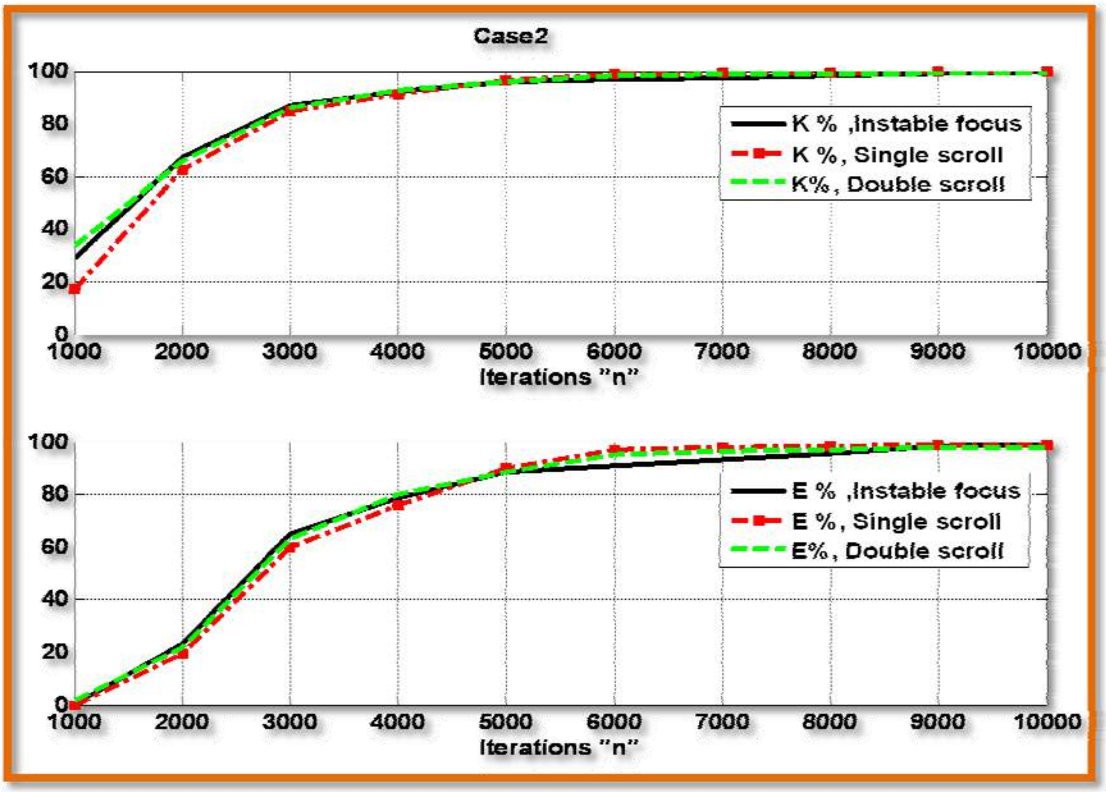

Figure 10: Performance indices K and E of the Chua's patterns versus time, case 2.

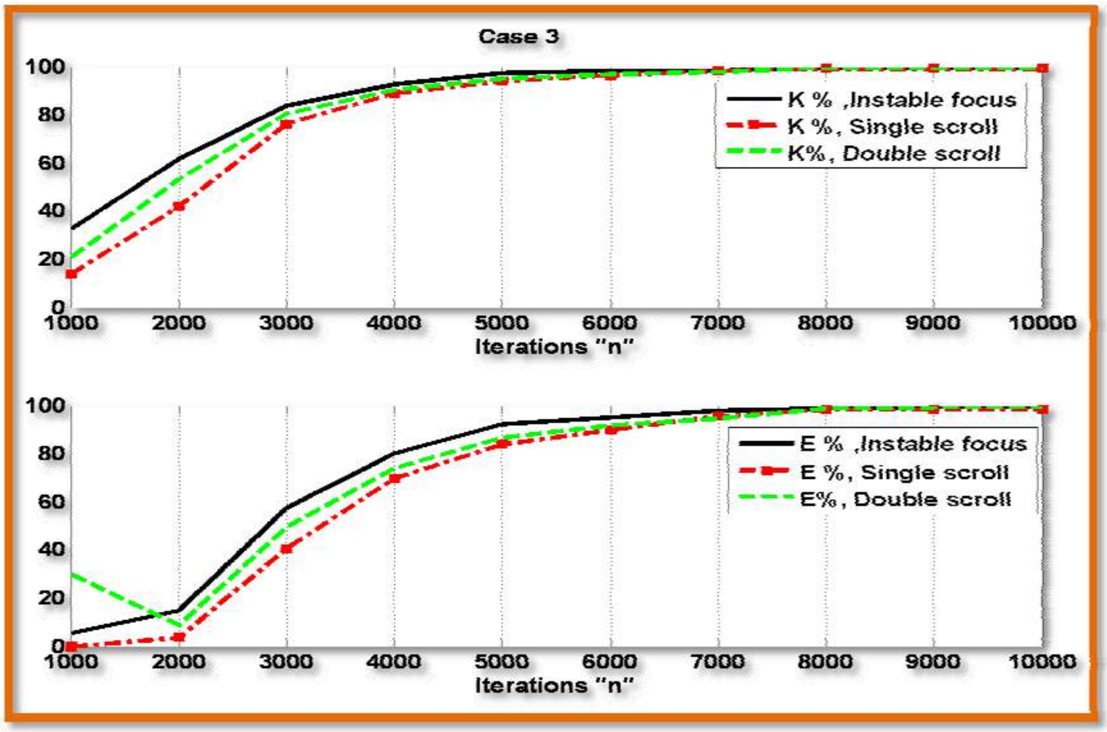

Figure 11: Performance indices K and E of the Chua's patterns versus time, case 3.

From Figures 9-11, we can deduce that instable focus plots are better than another two plots of chaos patterns (single scroll and double scroll) in achieving better area coverage (the performance index K, and E have more percentage value in various runtime), in the three specified cases.

5. Conclusion

The mobile robot trajectories generated by Chua's circuit signals either chaotic or non chaotic permits to ensure the fullest coverage of a rectangular workspace area for some particular parameter sets.

The coverage performance is measured by two different indexes namely a performance index K representing a ratio of areas that the trajectory passes through and an evenness index E which refers to how close in coverage each quarter of a rectangular workspace are. The enhancement techniques of coverage performance are performed by adjusting circuit parameters, mapping the appropriate state variables to robot's kinematic variables, in order to increase the coverage indexes.

It was shown that an instable focus, a non chaotic behavior of Chua's circuit, is also advantageous to provide good coverage performance of a mobile robot and is better than another two chaos patterns and this is the main contribution of this work. According to this study one can use simpler signals to generate complex trajectories of mobile robots and to guarantee better performances.

6. Acknowledgements

A very special thank you is due to Assistant Professor Dr. Supachai Vorapojpisut (*Thammasat University, Thailand*) for insightful comments, helping clarify and improve the manuscript.

7. References:

A. Jansri, K. Klomkarn, and P. Sooraksa. (2004). Further Investigation on Trajectory of Chaotic Guiding Signals For Robotics system. *In Proc. Int. Symp. Communication & Information Technology,* 1166-1170.

A. Jansri, K. Klomkarn, and P. Sooraksa. (2004). On Comparison of Attractors For Chaotic Mobile Robots *in Proc. 30th Annu. Conf. IEEE Industrial Electronics Society, IECON*, 3, 2536-2541.

A. Sekiguchi and Y. Nakamura. (1999). The Chaotic Mobile Robot. *In Proc. IEEE/RSJ. Int. Conf. Intelligent Robots and Systems,* (1), 172-178.

C. Chanvech, K. Klomkarn, and P. Sooraksa. (2006). Combined Chaotic Attractors Mobile Robots. *In Proc. SICE-ICASE Int. Joint Conf.*, 3079-3082.

J. Nicolas et al. (2003). A comparative Analysis of Evenness Index Sensitivity. *Int. Review Hydrobiology*, 88 (1), 3-15.

J. Palacin, J. A. Salse, I. Valganon, and X. Clua. (2004) Building A Mobile Robot For A Floor-cleaning Operation In Domestic Environments. *IEEE Transactions on Instrumentation and Measurement*, 53 (5), 1418–1424.

Leon O. Chua. (2007). Chua Crcuit. *Scholarpedia*, 2(10), 1488. L. S. Martins-Filho, R. F. Machado, R. Rocha, and V. S. Vale. (2004)

Commanding mobile robots with chaos. In ABCM Symposium Series in Mechatronics,J.C. Adamowski, E. H. Tamai, E. Villani, and P. E. Miyagi, EdsABCM, Rio de Janeiro, Brazil, 1, 40–46.

L.S. Martins et al., (2006). Kinematic Control of Mobile Robots To Produce Chaotic Trajectories. *ABCM Symposium Series in Mechatronics*, 2, 258-264.

M. Islam and K.Murase. (2005). Chaotic dynamics of a behavior-based miniature mobile robot: effects of environment and control structure. *Neural Networks*, 18 (2), 123–144.

P. Sooraksa and K. Klomkarn. (2010). No-CPU Chaotic Robots From Classroom To Commerce. *In IEEE circuits and systems magazine,* 10(1109), 46-53.

U. Nehmzow. (2003). Quantitative Analysis of Robot-Environment Interaction-Towards Scientific Mobile Robotics. *Robotics and Autonomous Systems*, 44 (1), 55–68.

S. Martins et al., (2007). Patrol Mobile Robots and Chaotic Trajectories. *In mathematical problems in engineering*, 2007, Article ID61543, 13 pages.

Y. Nakamura and A. Sekiguchi. (2001). Chaotic Mobile Robot. IEEE Transaction on Robotics and Automation, 17(6), 898–904.

Dr. Ashraf Anwar received his PhD degree in Electronics and Electrical Communication from Faculty of Engineering, Cairo University in 2005. Currently, he is an Assistant Professor at college of computers and Information Technology, Taif University. His research interests are mainly in the area of tracking system, control, and robotics.

Dr. Hedi Khammari received his PhD degree in Electrical Engineering from National School of Engineering, Tunis University in 1999. Currently, he is an Assistant Professor at college of computers and Information Technology, Taif University. His research interests are mainly in the area of nonlinear dynamics and the application of chaos theory in the field of communication, electric systems and bioinformatics.

Peer Review: This article has been internationally peer-reviewed and accepted for publication according to the guidelines given at the journal's website.